Soil Dynamics and Earthquake Engineering 105 (2018) 150–159

Contents lists available at ScienceDirect

Soil Dynamics and Earthquake Engineering

journal homepage: www.elsevier.com/locate/soildyn

# Numerical testing on wave-induced seabed liquefaction with a poro-elastoplastic model

Guan-lin Ye[a,*], Jian Leng[a], Dong-sheng Jeng[a,b]

[a] Department of Civil Engineering and State Key Laboratory of Ocean Engineering, Shanghai Jiao Tong University, Shanghai 200240, China
[b] Griffith School of Engineering, Griffith University Gold Coast Campus, Queensland 4222, Australia

ARTICLE INFO

*Keywords:*
Liquefaction
Wave
Seabed
Poro-elasto-plastic model
Effective stress

ABSTRACT

Dynamic seabed response under wave loading is one of key factors for the design and construction of offshore structures. Most previous studies were based on poroelastic seabed model. In this paper, based on a unified elasto-plastic constitutive model that can describe the liquefaction of sand and two-phase *u-p* theory for saturated soils, numerical tests are conducted to analyze the dynamic responses of a sandy seabed subjected to cyclic wave loads. The development of liquefaction zone, the change of excess pore water pressure (EPWP), the effective stress path, and the displacement vector are investigated. Numerical tests show that the proposed method is able to capture the mechanical behaviors of wave induced liquefaction of a sandy seabed. The calculated effective stress path and change of EPWP are similar to those of earthquake-induced liquefaction. In other words, the mechanism of wave-induced and earthquake-induced liquefaction are similar, despite of the loading forms. The liquefaction depth increases with the number of wave cycles. Meanwhile, a phase lag is observed between the liquefied seabed and wave motion. A comparison between the dynamic response of elastic and elasto-plastic seabed is presented to underline the importance of considering the plastic deformation of seabed.

## 1. Introduction

Wave-induced seabed liquefaction is an important topic in offshore geotechnical engineering, because seabed liquefaction can lead to the large deformation, even the failure of offshore structures such as, the continuous settlement of breakwaters in Niigata, Japan [29] and the failure of caisson in Barcelona Harbour, Spain [20]. Therefore, the dynamic response of seabed under wave loadings of the foundation structures, is one of the key factors to be considered in the design.

Two mechanisms of the wave-induced seabed liquefaction have been observed in the laboratory tests and field observations [35], depending on the manner of the pore pressure generated, namely, the oscillatory pore pressure and residual (accumulated) pore pressure. The oscillatory one is an ubiquitous response of porous material subjected to dynamic wave loading, which is always accompanied by the amplitude damping the phase lag. The residual one is the progressive nature of excess pore pressure, which is owning to the plastic deformation of seabed.

Several criteria for liquefaction have been suggested (e.g., Okusa, 1985; [35]; Tsai, 1995; [13]). It is generally accepted that the liquefaction occurs when the excess pore pressure becomes greater than the overburden soil pressure. The build-up of pore pressure under progressive and standing waves were observed in the wave flume tests and centrifuge tests [16,22]. In most experimental studies, only the pore pressure was measured by electronic transducers, the other factors, such as the effective stress paths and the stress-strain relations of soil elements, the deformation of the seabed cannot be captured due to the limitation in the monitoring technology. However, these deficiencies can be remedied by numerical analyses.

Numerous theoretical studies have been conducted to clarify the dynamic behaviors of seabed under wave loadings. Since the seabed is a saturated or almost saturated porous material, the Biot's poroelastic theory is widely applied in these studies. Analytical solution is an effective and idealized method to study the wave-induced dynamic response of the seabed (e.g., [11,27]). However, the analytical approach cannot deal with complex boundary conditions, which limits their capability. Therefore, finite element method (FEM) has been applied to investigate the seabed liquefaction in recent years (e.g., [18,17,9,38]). Sassa and Sekiguchi [22] proposed an elasto-plastic model considering the rotation of principal stress axes. The model was implemented into FEM to simulate the seabed responses subject to progressive and standing wave loadings. Based on the elasto-plastic model PZIII (Pastor et al., 1990) and the FEM code DIANA-SWANDYNE [14,42,7], and Ye et al. [33,34] conducted numerical studies of wave-induced

* Corresponding author.
*E-mail address:* ygl@sjtu.edu.cn (G.-l. Ye).

https://doi.org/10.1016/j.soildyn.2017.11.026
Received 9 August 2017; Received in revised form 26 October 2017; Accepted 24 November 2017

liquefaction around offshore structures. Recently, by using the COMSOL multi-physics software, Zhou et al. [39,40] analyzed the seabed liquefaction around pipelines under the wave and current loadings. To the knowledge of the authors, however, this kind of studies that treated the sandy seabed as an elasto-plastic material are still very limited.

In this paper, with a new constitutive model [36,37], which can describe the static/dynamic behavior of sands under various loading conditions in a unified way, effective stress based finite element analysis is carried out to study the dynamic response of a saturated seabed under the wave loading. A comprehensive discussion on the calculation results, including the development of excess pore water pressure (EPWP), the effective stress path and displacement of seabed, is conducted carefully to obtain the new insight into the wave-induced liquefaction.

## 2. Theoretical formulations

### 2.1. Elasto-plastic constitutive model for a porous seabed

The mechanical behaviors of sand are dependent not only on the shape of particles, angular or round, but also on its density, the experienced strain history, and even on the degree of structure formed in its deposition. Sand may behave totally differently under different loadings and drained conditions. For instance, when subjected to undrained cyclic loading, loose sand will be liquefied without transition from contractive to dilative state, while for medium dense sand liquefaction with cyclic mobility occurs. On the other hand, for dense sand the liquefaction will never occur. Loose sand subjected to cyclic loading will be liquefied under un-drained condition but may be compacted to a denser state under drained condition. Based on the concepts of subloadings [8] and super-loading [1,30,36,37] proposed a new constitutive soil relations called as Cyclic Mobility model (short for CM model). The CM model is able to describe the mechanical behavior of soils not only under monotonic loading, but also under dynamic loading, which very few constitutive models can perform well. In addition, the CM model can describe the cyclic behaviors of saturated sands with different densities using the same set of material parameters. The values of material parameters depend on what kind of sands it deals with rather than the density. The number of material parameters involved in the proposed model is only eight which will be introduced later, thus it is easy to be applied in numerical analysis. A brief description of the yield surfaces is presented in Fig. 1(a).

Two state variables, (i) $R^*$, the similarity ratio of the super-loading yield surface to normal yield surface, and (ii) $R$, the similarity ratio of the super-loading yield surface to sub-loading yield surface, are defined in the same way as those in Asaoka et al. [1]. Definition of these variable are given as the follows:

$$R^* = \frac{\widehat{p}}{\bar{p}} = \frac{\widehat{q}}{\bar{q}}, \quad 0 < R^* \le 1 \quad and \quad \frac{\widehat{q}}{\widehat{p}} = \frac{\bar{q}}{\bar{p}} \tag{1}$$

$$R = \frac{p}{\bar{p}} = \frac{q}{\bar{q}}, \quad 0 < R \le 1, \quad and \quad \frac{\bar{q}}{\bar{p}} = \frac{\widehat{q}}{\widehat{p}} = \frac{q}{p}, \tag{2}$$

where $(p,\ q)$, $(\widehat{p},\ \widehat{q})$ and $(\bar{p},\ \bar{q})$ represent the present stress state, the corresponding normally consolidated stress state and the structured stress state on the *p-q* plane, respectively. The present stress state is always situated on the sub-loading surface, which is given in the following form:

$$f = \ln\frac{\sigma_m}{\sigma_{m0}} + \ln\frac{\mathrm{M}^2 - \zeta^2 + \eta^{*2}}{\mathrm{M}^2 - \zeta^2} + \ln R^* - \ln R - \frac{\varepsilon_v^p}{\mathrm{C_p}} = 0 \tag{3}$$

In Eq. (3), $\sigma_m = \frac{1}{3}\sigma_{ii}$ is the mean effective stress, and $\sigma_{m0} = 98.0$kPa is a reference stress. $\zeta = \sqrt{\frac{3}{2}\beta_{ij}\beta_{ij}}$ is an anisotropic state variable, with $\beta_{ij}$ as the anisotropic stress tensor. $\eta^* = \sqrt{\frac{3}{2}\hat{\eta}_{ij}\hat{\eta}_{ij}}$ represents the difference between the stress ratio tensor $\eta_{ij}$ and the anisotropic stress tensor $\beta_{ij}$, in which

$$\hat{\eta}_{ij} = \eta_{ij} - \beta_{ij},\ \eta_{ij} = \frac{S_{ij}}{\sigma_m},\ S_{ij} = \sigma_{ij} - \sigma_m\delta_{ij} \tag{4}$$

where $S_{ij}$ is the deviatoric stress tensor, and $\delta_{ij}$ is Kronecker delta tensor. In Eq. (3), $\mathrm{C_p}$ is expressed as:

$$\mathrm{C_p} = \frac{\lambda - k}{1 + e_0}, \tag{5}$$

where λ and κ are the compression and swelling index, and $e_0$ is a reference void ratio at a reference stress $\sigma_{m0} = 98.0$ kPa.

In this model, the gradient of the Critical State Line (C.S.L.) is assumed to be constant. Fig. 1(b) shows the yielding surfaces and its change in the flat ratio of the elliptical yield surface due to the anisotropy. The third state variable introduced in the model, $\zeta$, the stress-induced anisotropy, is assumed that the larger $\zeta$ is, the larger the eccentric ratio of the ellipse will be.

An associated flow rule is employed in the model:

$$d\varepsilon_{ij}^p = \Lambda\frac{\partial f}{\partial \sigma_{ij}} \tag{6}$$

The consistency equation for the sub-loading yield surface can then be given as:

$$df = 0 \Rightarrow \frac{\partial f}{\partial \sigma_{ij}}d\sigma_{ij} + \frac{\partial f}{\partial \beta_{ij}}d\beta_{ij} + \frac{1}{R^*}dR^* - \frac{1}{R}dR - \frac{1}{C_p}d\varepsilon_v^p = 0 \tag{7}$$

The evolution rule for the degree of structure, $R^*$, is defined as:

$$dR^* = U^* d\varepsilon_d^p,\ U^* = \frac{a\mathrm{M}}{\mathrm{C_p}}R^*(1 - R^*)\ (0 < R^* \le 1), \tag{8}$$

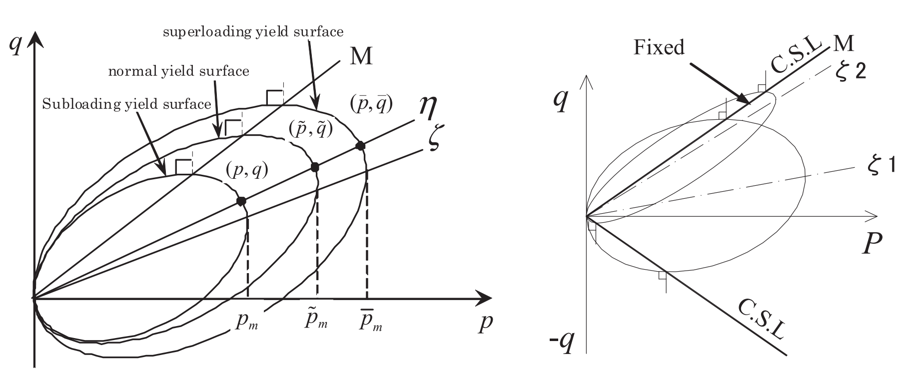


(a) Subloading, normal and superloading yield surfaces at different $\zeta$

(b) Changes of subloading yielding surface

**Fig. 1.** Yield surfaces in *p-q* plane.